ELECTRICAL ENGINEERING AND ENERGY

OPEN ACCESS

HPPC Derived Feature Augmented DNN for SOC Estimation in Electric Vehicles

Abdulkadir Mühendis[1], and Ramazan Akkaya[2]

[1] 13713 Al-Khalidiya, Diriyah, Riyadh, Saudi Arabia
[2] Dept. of Electrical and Electronics Engineering, Konya Technical University, Konya, Türkiye

Submitted: 26 February 2026
Accepted: 17 April 2026
Online First: 18 April 2026

Corresponding author
Abdulkadir Mühendis,
e208121001001@ktun.edu.tr

DOI:10.64470/elene.2026.28

Abstract: Accurate State of Charge (SOC) estimation is a critical function for ensuring the safety, performance, and longevity of lithium-ion batteries used in electric vehicles. Traditional model-based estimation methods—such as coulomb counting and Kalman filtering—often suffer from cumulative errors, parameter drift, and poor adaptability under varying temperature and dynamic load conditions. In contrast, data-driven approaches provide a promising alternative by learning complex nonlinear relationships directly from experimental data without relying on predefined equivalent circuit or electrochemical models. This study introduces an HPPC-derived feature-augmented deep neural network (DNN) framework that leverages the strengths of data-driven learning for accurate and robust SOC estimation. The proposed DNN is trained exclusively on Hybrid Pulse Power Characterization (HPPC) data and enhanced through feature engineering that captures voltage recovery dynamics, internal resistance, and temperature effects. Unlike conventional HPPC-based approaches, the model demonstrates strong generalization by accurately predicting SOC during EPA Urban Dynamometer Driving Schedule (UDDS) cycles—despite no exposure to driving-cycle data during training. Experimental validation on a 14-cell lithium-ion battery pack, managed by an L9963E-based battery management system, shows that the proposed model achieves a root mean square error (RMSE) reduction of 0.72% compared to traditional estimation techniques. These results confirm that data-driven DNN models trained on HPPC-derived features can offer high-accuracy, scalable, and generalizable SOC estimation solutions suitable for real-time deployment in next-generation automotive battery management system (BMS) platforms.

Keywords Battery management, deep neural networks, HPPC characterization, SOC estimation, UDDS driving cycles

1. Introduction

Lithium-ion batteries (LiBs) have become the cornerstone of modern electrification, powering electric vehicles (EVs), portable electronics, and renewable energy storage systems due to their high energy density, long cycle life, and stable performance. Ensuring the safe, reliable, and efficient operation of LiBs depends critically on accurate SOC estimation, a parameter that directly influences range prediction, energy

efficiency, and battery safety in battery management systems (Carrera et al., 2025). Conventional SOC estimation methods—such as coulomb counting, open-circuit voltage (OCV) measurement, equivalent circuit models (ECMs), and Kalman filtering—have been widely adopted in industrial BMS implementations. However, these model-based approaches are often limited by cumulative measurement errors, dependence on parameter identification, and sensitivity to environmental variations such as temperature and load dynamics. In practice, these factors lead to error propagation and poor adaptability when batteries operate under complex, real-world driving profiles.

Recent advances in data-driven modeling have opened new avenues for SOC estimation. Techniques based on artificial intelligence (AI), particularly deep neural networks (DNNs), can teach nonlinear, time-dependent relationships between measurable battery parameters (voltage, current, temperature) and SOC directly from experimental data. These approaches eliminate the need for explicit electrochemical modeling or circuit parameterization, offering a scalable solution adaptable to different battery chemistries and conditions (Fang et al., 2021). Nevertheless, the performance and generalization of DNN-based SOC estimators are strongly influenced by the quality, diversity, and representativeness of the training data. To address this challenge, the Hybrid Pulse Power Characterization (HPPC) protocol provides a systematic method for collecting comprehensive datasets that capture voltage recovery, internal resistance variation, and temperature-dependent behavior across the full SOC range. HPPC-derived data form a robust foundation for developing generalizable data-driven models that remain accurate beyond laboratory conditions (Zheng & Luo, 2024). However, while HPPC-based training ensures controlled coverage of battery dynamics, it remains uncertain whether models trained solely on HPPC data can generalize effectively to realistic driving cycles such as those defined by the U.S. Environmental Protection Agency (EPA), including the UDDS (Z. Ren & Du, 2023). In this context, this study presents a data-driven, HPPC-derived feature-augmented DNN framework for accurate SOC estimation of lithium-ion batteries. The proposed model is trained exclusively on HPPC datasets collected from a 14-series-cell (14S1P) lithium-ion battery pack managed by an L9963E-based BMS and enhanced with feature engineering techniques that extract electrochemical characteristics such as internal resistance and voltage relaxation behavior. The model's generalization capability is rigorously evaluated against EPA UDDS driving profiles, demonstrating that accurate SOC estimation can be achieved without retraining on driving-cycle data. Comparative analysis reveals that the proposed DNN significantly outperforms traditional estimation techniques in terms of accuracy, robustness, and computational efficiency, highlighting the transformative potential of data-driven approaches for next-generation BMS.

2. Materials and Methods

2.1 Experimental and Methods

This study utilizes a 14-series-cell (14S1P) lithium-ion battery pack constructed from ASPİLSAN INR18650A28 cylindrical cells, each with a nominal voltage of 3.65 V and a rated capacity of 2.8 Ah, governed by an L9963E-based BMS from STMicroelectronics. To comprehensively characterize battery behavior, a series of charge and discharge cycles were performed under varying ambient temperatures (−20 °C, 0 °C, 25 °C, and 50 °C) and C-rates (0.05C, 0.1C, 0.25C), adhering to manufacturer's specifications and thermal limitations. The following Figure 1 shows the real experimental equipment, cylindrical cells structure, connected loads and tools.

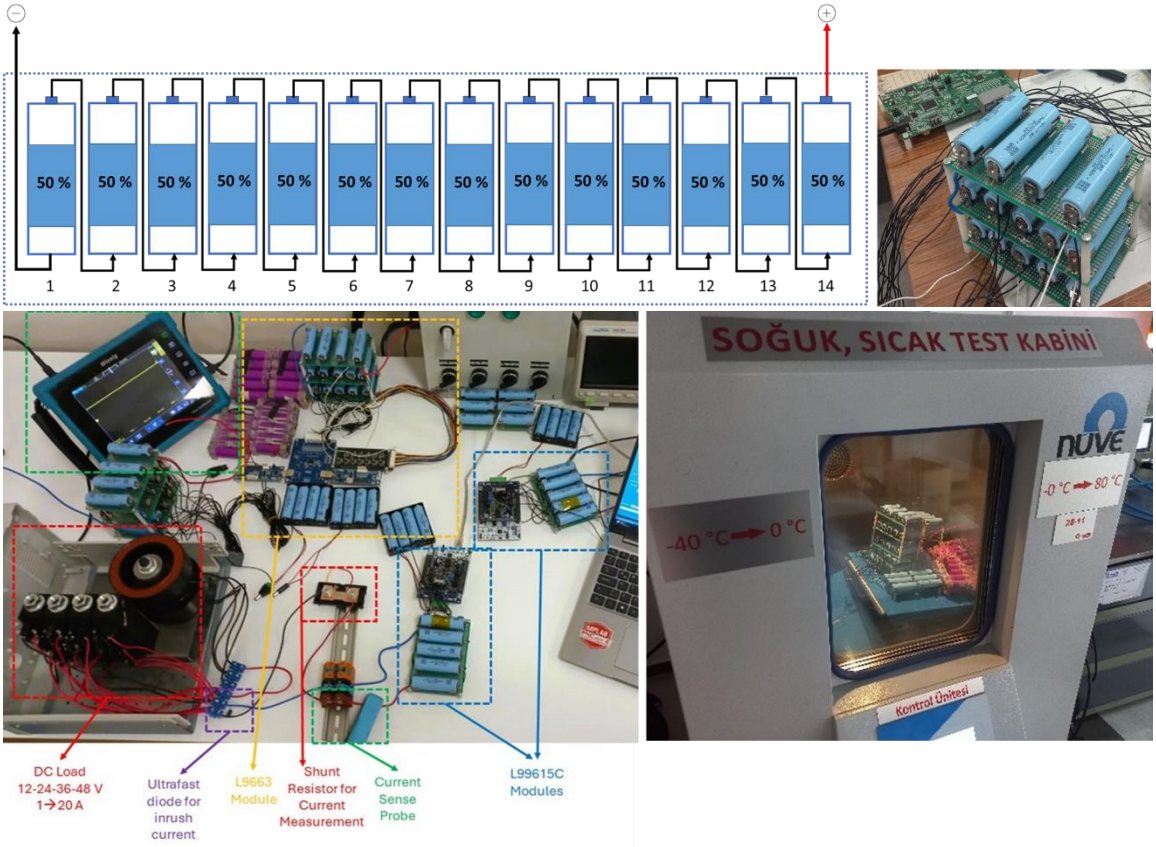

Figure 1 Experimental Setup

The C-rate refers to the charge or discharge current relative to the battery's capacity considering all temperature limitations. A 1C rate means the battery is discharged in one hour, while a 0.5C rate indicates discharge over two hours (Miao et al., 2022). The following Table 1 shows the performance specification of those cells. Manufacturers highly recommended these specifications and thermal limitations to avoid any failure modes during the test.

Table 1. Performance specification for INR18650A28 cells

ASPILSAN Datasheet Limitations			
Nominal	Discharge capacity	2800	mAh
	Nominal Voltage	3,65	V
	Initial AC Impedance	<= 20	mΩ
Charge	Charge Current	1400	mA
	Max Charge Current	4000	mA
	End voltage	4,2	V
	Cut-off Current	140	mA
Discharge	Discharge Current	560	mA
	Max Discharge Current	14000	mA
	Max Conditional Discharge Current (SOC > 70 %)	25000	mA
	End Voltage	2,5	V

2.2 Battery Management Unit L9963E

The battery pack was monitored and controlled using an L9963E-based BMS from STMicroelectronics, which is presented in the following Figure 2. This module provides per-cell voltage monitoring, pack current measurement, and multiple NTC thermistor inputs for temperature sensing (Wassiliadis et al., 2021). L9963E provides high-precision voltage measurement (±5 mV accuracy) and current measurement (±0.1 A accuracy) (Mühendis & Akkaya, n.d.-b).

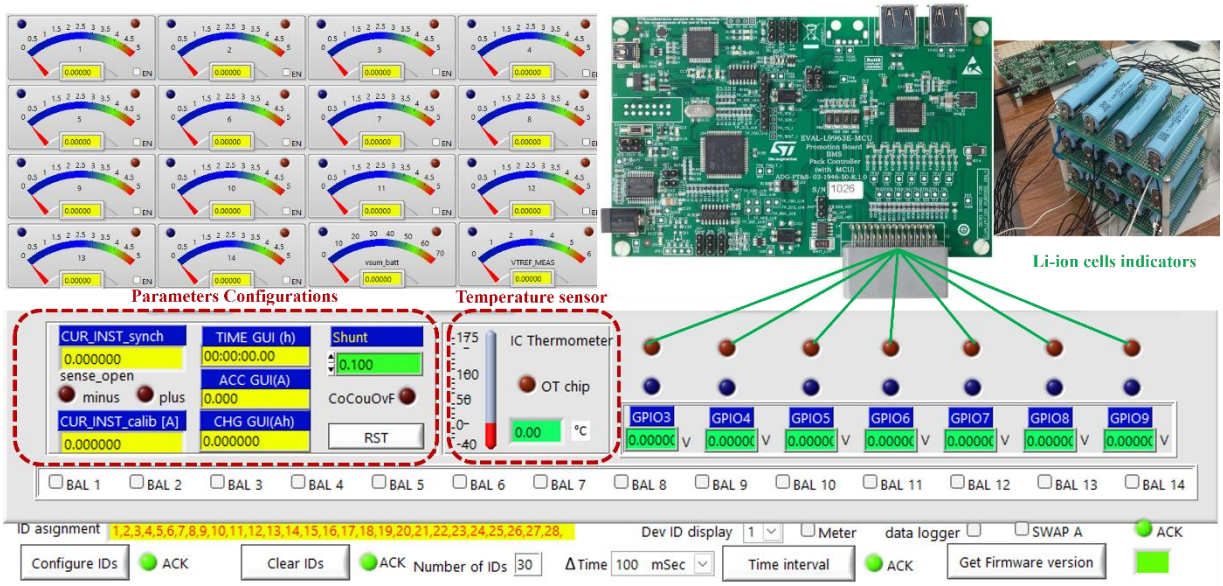

Figure 2 L9963E Data acquisition module

In this study, an external active balancing module was additionally integrated to minimize cell-to-cell SOC divergence under high-load test conditions (Chandran et al., 2021). Voltage, current, temperature, and time-stamp data were sampled at 1 Hz and recorded using both an SPC574S64E3 automotive-grade microcontroller and a NI-based GUI interface for visualization and backup logging (Hannan et al., 2020). Synchronization between voltage and current sampling was ensured by aligning voltage conversion requests from the L9963E with the coulomb-counting routine in the microcontroller, minimizing phase error and improving dynamic response fidelity (Mühendis & Akkaya, 2025).

2.3 Testing Method

Dynamic characterization employed the HPPC protocol to elicit transient responses across the SOC range. HPPC sequences were executed at SOC steps from 10% to 90% in 10% increments. At each SOC step, a short high-current discharge pulse was applied immediately followed, after a brief rest, by a corresponding charge pulse; pulse polarity, amplitude and duration were selected to emulate realistic transient loading while avoiding significant SOC drift. In this study, pulses were 10 S in duration with amplitude set to 1C (Standardized tests, such as those defined by FreedomCAR or IEC 62660, typically use short pulses, often 10 seconds for discharge and 10 seconds for charge, to simulate accelerating and regenerative braking), followed by rest/recovery intervals to allow terminal voltage relaxation toward quasi-equilibrium; each SOC point was repeated for three HPPC runs to capture hysteresis and cycle-dependent effects (Harper et al., 2023). These pulse parameters were chosen to balance sensitivity to dynamic impedance features with thermal and safety constraints of the cells. Where required, additional shorter or lower-amplitude pulses were applied to probe specific dynamic regimes; all pulse schedules and timings are archived in the supplementary materials. Prior to testing, all measurement channels were calibrated against laboratory

reference instruments and synchronization between current and voltage conversions was validated by coordinating L9963E conversion requests with the microcontroller managed coulomb counting routine to minimize phase error. Measurements are summarized in the following Table 2 where the raw test data were stored securely and backed up after each test campaign; subsequent preprocessing steps (filtering, normalization, feature extraction and labeling) were applied offline to generate the training, validation and test sets used for DNN development (JiaQi et al., 2024).

Table 2. Cell capacity (Ah) measured at temperatures from −20°C to 50°C for charge/discharge cycles

Temperature (^{0}C)	Charge Cycles		Discharge cycles		
	Capacity (Ah)		Capacity (Ah)		
	0,05 C	0,1 C	0,05 C	0,1 C	0,25 C
-20	1,97	3,83	1,72	3,11	9,02
0	2,06	4,01	1,86	3,56	9,43
25	2,19	4,19	2,03	3,94	9,69
50	2,33	4,27	2,27	4,07	9,82

The measured current is integrated over time to calculate the total charge that has flowed. Fully synchronized current and voltage samples with 200 mA passive internal balancing current for each cell in both normal and silent-balancing modes (Wu et al., 2016). This technique is performed to evaluate the charge mode during vehicle operations considering driving condition variations (Majasan et al., 2021). The current sensing interface used for coulomb counting is also capable of detecting failures such as open wires and overcurrent in sleep mode (Obuli Pranav et al., 2024). The cell balancing terminals can detect any open or short circuit faults whereas the internal power MOSFETs are protected against overcurrent or in rushed current signals as well (Pop et al., 2005). The embedded SPC574S64E3 microcontroller can evaluate the charge variations ΔQ in the battery pack, by referring to a known previous state of charge Q(t0) and implementing the following algorithm:

$$Q(t) = Q(0) + \int_0^t I(\tau).d\tau \tag{1}$$

$$SOC = \left(\frac{Q_{accumulated}}{Q_{capacity}}\right) * 100 \tag{2}$$

$$SOC = SOC(t_0) + \frac{1}{C_{rated}} \int_{t_0}^{t_0+\tau} (I_b - I_{loss})dt \tag{3}$$

2.4 Data Collection

Data collection focuses on generating a high-quality, reproducible dataset that captures the battery pack's electrochemical response across SOC, temperature, and load conditions (F. Liu et al., 2016). HPPC test sequences were executed at SOC steps of 10%–90% (10% increments) and repeated three times per SOC point to capture hysteresis and cycle dependence. At each SOC step a calibrated discharge pulse was applied, followed by a rest period and a corresponding short charge pulse when required by the HPPC schedule (Xiao et al., 2024). In addition to HPPC runs, steady CC/CV charge and CC discharge sequences at 0.05C, 0.1C and 0.25C and environmental temperatures of −20 °C, 0 °C, 25 °C and 50 °C were recorded to enrich the dataset (Mühendis & Akkaya, 2025).

The error of the integration plays a huge role in SOC estimation and depends on the initial SOC estimation as well (Wassiliadis et al., 2021; Wu et al., 2016).

$$SOC_{(t)} = SOC_{(t-1)} \cdot \int_{t-1}^{t} \frac{I_t \cdot \eta}{Q_n} dt \quad (4)$$

$$\frac{dSOC}{dt} = -\frac{i}{3600A_h(T)} \quad (5)$$

$$\frac{dV_1}{dt} = \frac{i}{C_1(SOC,T)} - \frac{V_1}{R_1(SOC,T).C_1(SOC,T)} \quad (6)$$

$$V_t = V_0(SOC, T) - iR_0 - V_1 \quad (7)$$

$$f(x, i) = \begin{bmatrix} x = [SOC\ V_1]^T \\ -\frac{i}{3600A_h(t)} \\ -\frac{i}{C_1(SOC,T)} - \frac{V_1}{R_1(SOC,T).C_1(SOC,T)} \end{bmatrix} \quad (8)$$

$$h(x, i) = V_0(SOC, T) - iR_0 - V_1 \quad (9)$$

HPPC method aims to extract available charge and discharge power. The following Figure 3 shows the developed ECU to be used as HPPC tester by controlling the pulses width using the embedded Stm32f103 which connected with automotive grade output MOSFETs (W. Liu et al., 2022a). The maximum discharge or charge power is presented as below:

Figure 3 L9963E Data acquisition module

$$P_{max} = \frac{(V_{OCV} - V_{limit}) * V_{limit}}{R_{internal}} \quad (10)$$

The HPPC method is a cornerstone of battery characterization in BMS, providing essential data for power prediction, state estimation, and thermal management (Tong et al., 2016). By simulating real-world conditions, it ensures the BMS optimizes battery safety, efficiency, and longevity (Frendo et al., 2020). Despite its time and cost demands, its standardized approach and integration with advanced modeling tools make it indispensable for EV battery development and management (W. Liu et al., 2022b).

In this study, essential electrochemical parameters—including instantaneous resistance, dynamic resistance, OCV– SOC relationships, and polarization time constants—were extracted and integrated into the estimation algorithm. Input features were derived from the HPPC protocol data to capture the complex

interdependence among C-rate, temperature, and SOC (Yuan et al., 2025). All features were pre-processed to normalize their ranges and enhance model robustness under varying operational conditions. When multiple cells are connected in series, the total pack voltage equals the sum of the individual cell voltages. Consequently, variations in C-rate and temperature at the cell level collectively influence the overall performance of the battery pack (Naha et al., 2020). A high C-rate under low-temperature conditions can induce a pronounced voltage drop across the pack (El Fallah et al., 2024). In such cases, cell balancing becomes essential, as any mismatch in cell characteristics may result in uneven discharge, accelerating the degradation of weaker cells (Mühendis & Akkaya, n.d.-a). Furthermore, temperature profoundly affects electrochemical behaviour and overall performance. Elevated temperatures can accelerate aging mechanisms, reduce capacity, and raise safety risks. Figure 4 illustrates the discharge characteristics under various temperature and C-rate conditions.

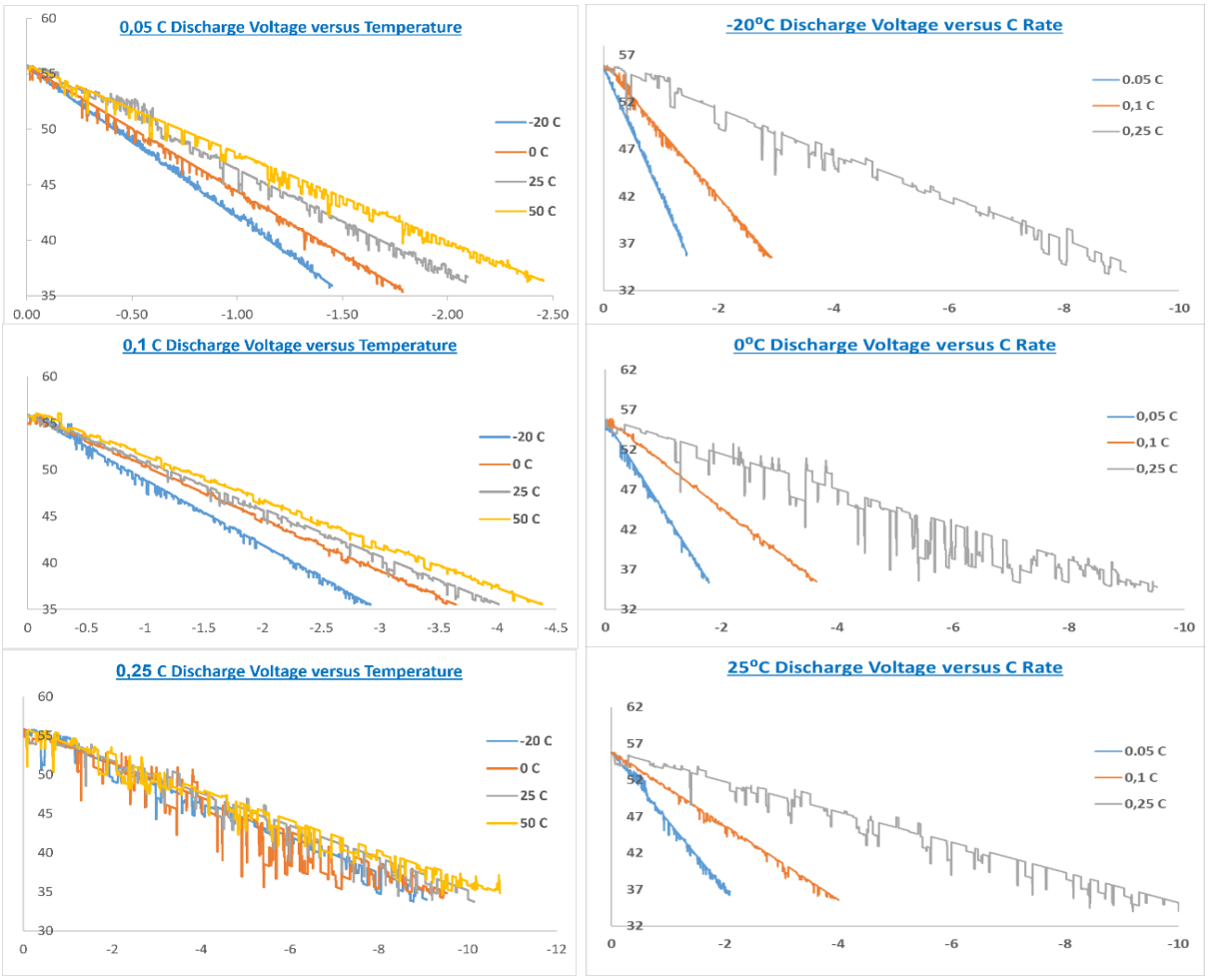

Figure 4 Discharge voltage versus Temperature/Cycles curves

Discharging a battery at higher C-rates yields a reduced apparent capacity compared to operation at lower discharge rates. This effect, commonly referred to as capacity offset, arises from increased internal energy losses as SOC with elevated current flow (Tran et al., 2022). At higher discharge rates, the internal resistance of the cell becomes more pronounced, leading to larger voltage drops and enhanced heat generation. Consequently, examination of the discharge voltage curve provides valuable insight into internal resistance characteristics and their influence on overall battery performance (Eleftheriadis et al., 2023).

Both C-rate and temperature are critical parameters influencing the discharge characteristics of lithium-ion batteries (Murnane & Ghazel, n.d.). Higher C-rates result in steeper voltage drops, shorter plateau regions, and lower apparent capacity, accompanied by increased heat generation. Temperature extremes further modulate these effects: low temperatures reduce available capacity and elevate internal impedance, whereas high temperatures—particularly under high C-rate conditions—intensify thermal management challenges (Obisakin & Ekeanyanwu, 2022).

Understanding these effects is essential for developing accurate SOC estimation algorithms and reliable BMS for electric vehicles (Lelie et al., 2018). At very low temperatures, cells often struggle to deliver sufficient power at high C-rates, leading to voltage sag and premature cutoff (Hossain Lipu et al., 2020). Higher C-rates accelerate the discharge process, generating more heat and adversely affecting both performance and safety (Tran et al., 2022). Conversely, low-temperature conditions reduce capacity and increase internal resistance, further challenging battery efficiency and stability.

Balancing the C-rate with cell temperature is critical to achieving an optimal charge profile (Ghaeminezhad et al., 2023). At low temperatures, lithium-ion cells exhibit reduced capacity and increased internal resistance, causing high C-rates to have a more pronounced adverse effect on capacity readings (Wang et al., 2023). Conversely, at elevated temperatures, cell capacity improves and internal resistance decreases, resulting in a diminished impact of high C-rates on the measured capacity (Wang et al., 2023). Figure 5 illustrates the charge voltage profiles across various C-rate cycles.

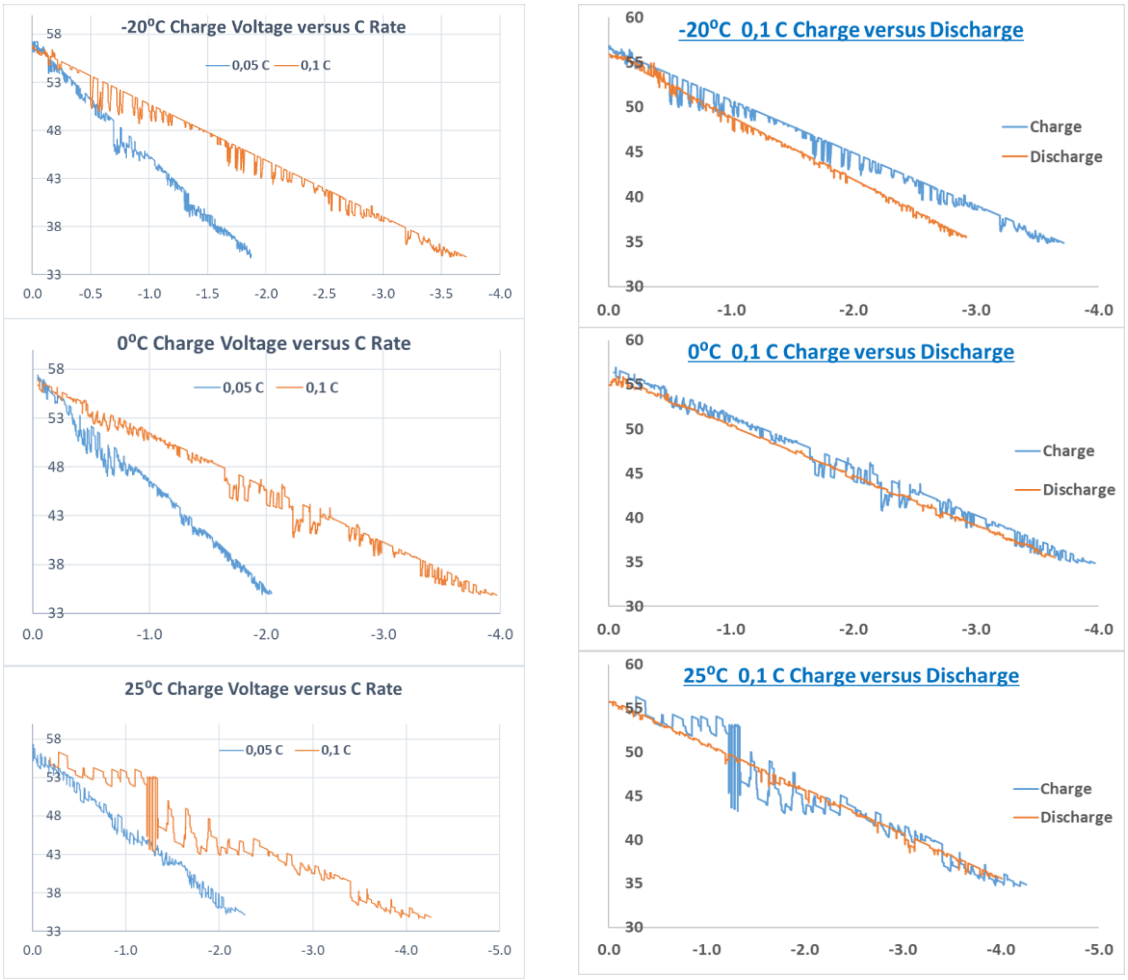

Figure 5 Charge voltage versus Temperature/Cycles curves

When 14 cells are connected in series, the effects of C-rate and temperature become more pronounced (Ko & Choi, 2021). A single underperforming cell can influence the entire string, resulting in reduced overall performance and accelerated degradation (Dai et al., 2021a). The C-rate strongly affects both the charging and discharging behaviors of lithium-ion cells (Xiong et al., 2017).

$$V_{oc} = OCV(SOC) - I(t).R_{int}(SOC,T) \quad (11)$$

2.5 Data Preprocessing and labeling

A precise understanding of the SOC-OCV relationship is fundamental to battery management systems. This correlation is highly nonlinear and dependent on battery chemistry, temperature, and age (H. Ren et al., 2019a). In this work, the SOC-OCV function is determined experimentally by fitting a curve to data from controlled charge/discharge tests. Figure 6 illustrates the combined effect of SOC-OCV during charge/discharge cycles.

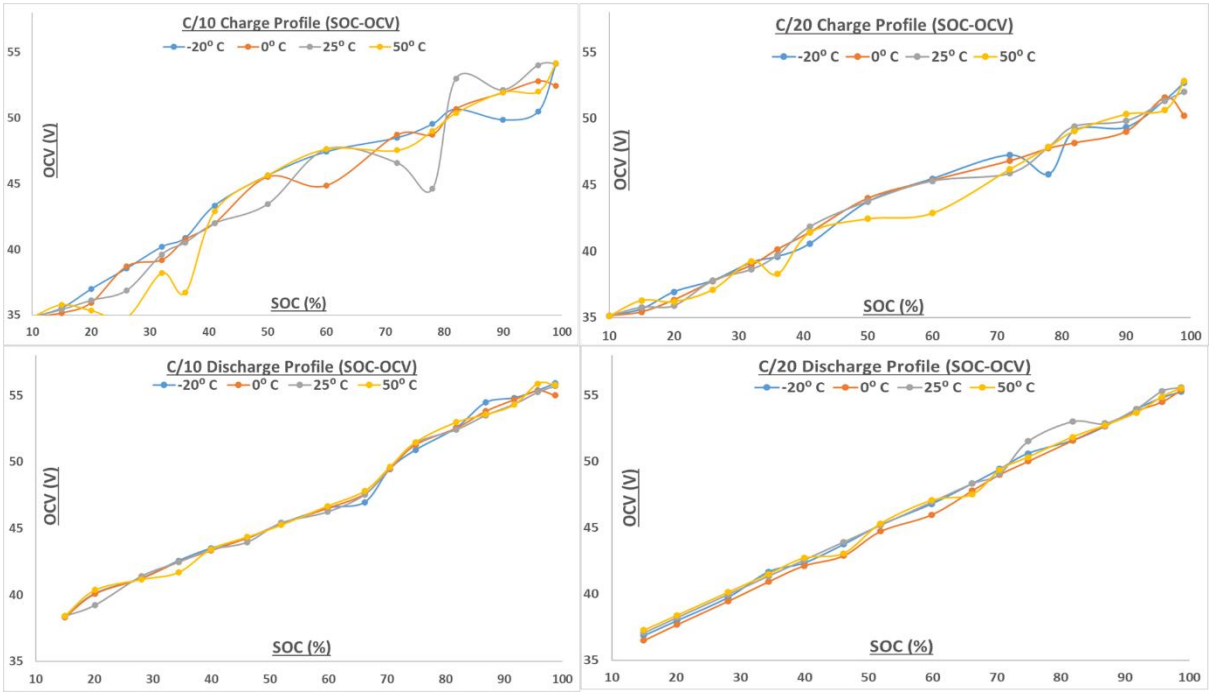

Figure 6 The combined effect of SOC-OCV during charge/discharge cycles

The fidelity of any SOC estimation algorithm is fundamentally dependent on the quality of the underlying battery characterization data. To this end, the HPPC test is a widely adopted and effective protocol (Jin et al., 2021). Its strength lies in its ability to capture essential electrochemical and dynamic characteristics, such as internal impedance, under controlled yet representative load profiles (MÜHENDİS & KULAKSIZ, 2020). For the data to be robust, HPPC characterization must be performed across a comprehensive range of operating temperatures and C-rates, followed by systematic data preprocessing to ensure accuracy (Hu et al., 2019). The rich dynamic information contained within these responses, such as the voltage recovery slope and the precise SOC change during each pulse, provides critical time-series features (Dai et al., 2021b). These features are leveraged as vital training inputs for the Deep Neural Network (DNN), enabling it to learn the complex, nonlinear mapping between the battery's external measurements and its internal SOC (Yang et al., 2021).

The methodological approach began with feature engineering from HPPC test data, which key parameters such as internal resistance, SOC-OCV curves, and polarization time constants were extracted. These features

were then subjected to a comprehensive preprocessing pipeline which included noise filtering, time-series synchronization, and temperature compensation (H. Ren et al., 2019b). The reference SOC, used as the target label for supervised learning, was computed via coulomb counting with OCV-based correction. After all features were normalized to a [0, 1] range, the dataset was partitioned into training (70%), validation (15%), and testing (15%) subsets. To ensure temporal generalization and prevent overfitting, this division was performed on entire cycles, guaranteeing that the model was validated and tested on chronologically unseen data. The following Figure 7 shows charge/discharge profiles based on SOC cycles. The HPPC test allows for the direct calculation of internal resistance components from the voltage response to a current pulse. This represents the immediate voltage drop due to the bulk resistance of the electrolyte, electrodes, and contacts (Mühendis & Akkaya, n.d.-b). Now the current pulse I is applied as the following equation:

$$R_0 = \frac{\Delta V_{inst}}{I} = \frac{|V(t_0^+) - V(t_0^-)|}{I} \quad (12)$$

where; $V(t_0^+)$: The voltage immediately before the current pulse, $V(t_0^-)$: The voltage at the instant the current pulse begins, I: The magnitude of the discharge current pulse

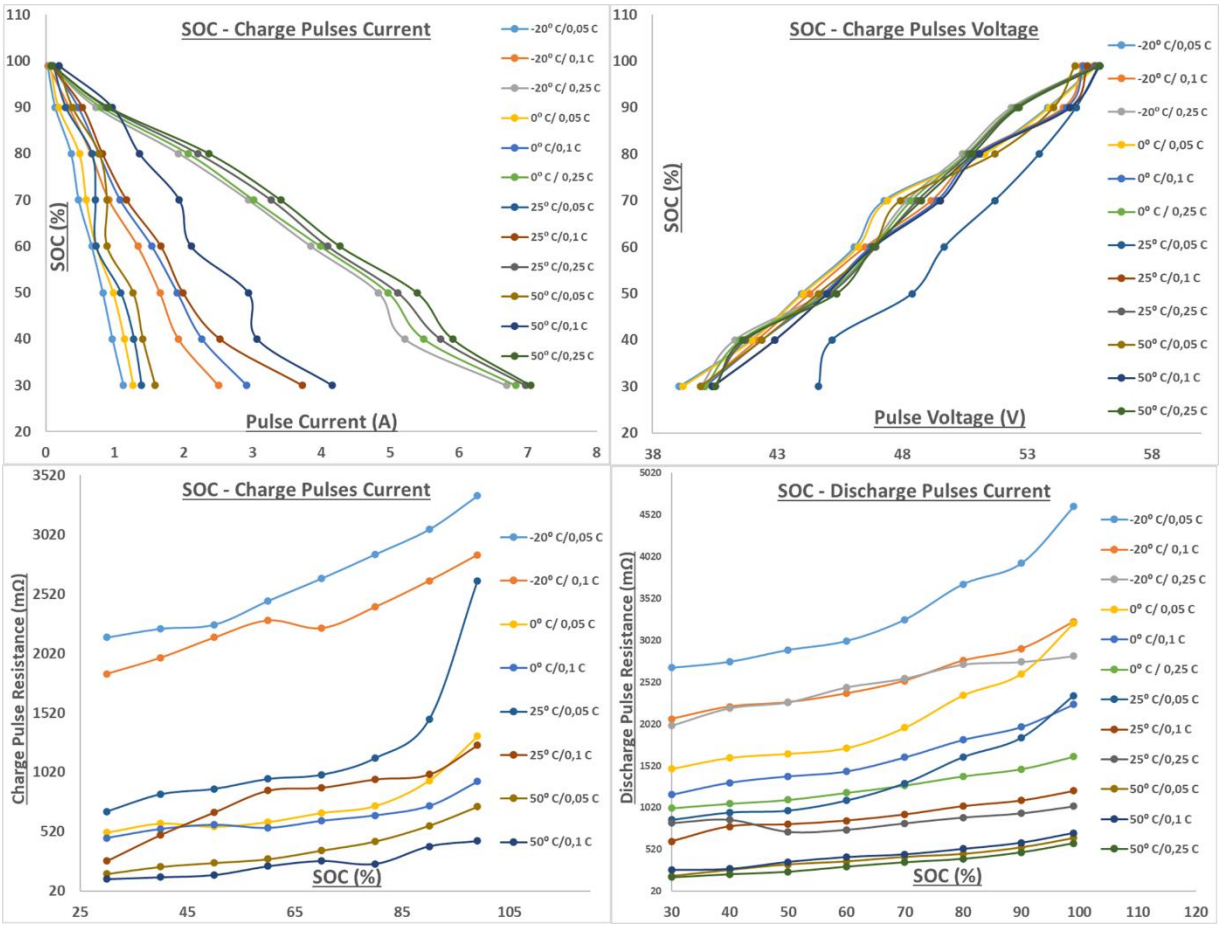

Figure 7 SOC-Charge/Discharge profiles

2.6 Deep Neural Network Architecture

The deep neural network (DNN) was designed for accurate SOC prediction using the HPPC dataset, leveraging five input features: time, cycle, current, voltage and temperature selected for their ability to capture temporal and aging dynamics of lithium-ion batteries (El Maliki et al., 2024). The presence of too many neurons will present a risk of over-fitting, while too few neurons will underfit the data.

The network was implemented using the TensorFlow framework in Python and trained on a workstation equipped with an NVIDIA Quadro P2200 GPU to ensure computational efficiency. The Adam optimizer was employed with an initial learning rate of 0.001, a batch size of 64, and a maximum of 500 training epochs. An early-stopping mechanism with a patience of 20 epochs was applied to prevent overfitting by halting training once the validation loss plateaued. The loss function was defined as the mean squared error (MSE) between the predicted and reference SOC values. Hyperparameters, including learning rate, number of neurons per layer, and dropout rate, were tuned based on validation performance. The training process was repeated five times with random weight initialization, and the average performance was reported to ensure statistical reliability.

The architecture of this neural network has been designed carefully by comprising three hidden layers with 16, 12 and 5 neurons, respectively, using ReLU activation to model non-linear relationships, followed by a single output layer with sigmoid activation to predict SOC. When combined with rigorous preprocessing and robust modelling techniques, HPPC-derived data enables highly accurate, adaptable, and reliable SOC estimation frameworks.

$$y_i = F(u_i) = F\sum_i \omega_{ji} x_i + b_j \tag{13}$$

Model training was conducted on an NVIDIA Quadro P2200 GPU to ensure computational efficiency. The training configuration included the mean squared error (MSE) as the loss function and the Adam optimizer. The following Figure 8 shows the proposed DNN architecture.

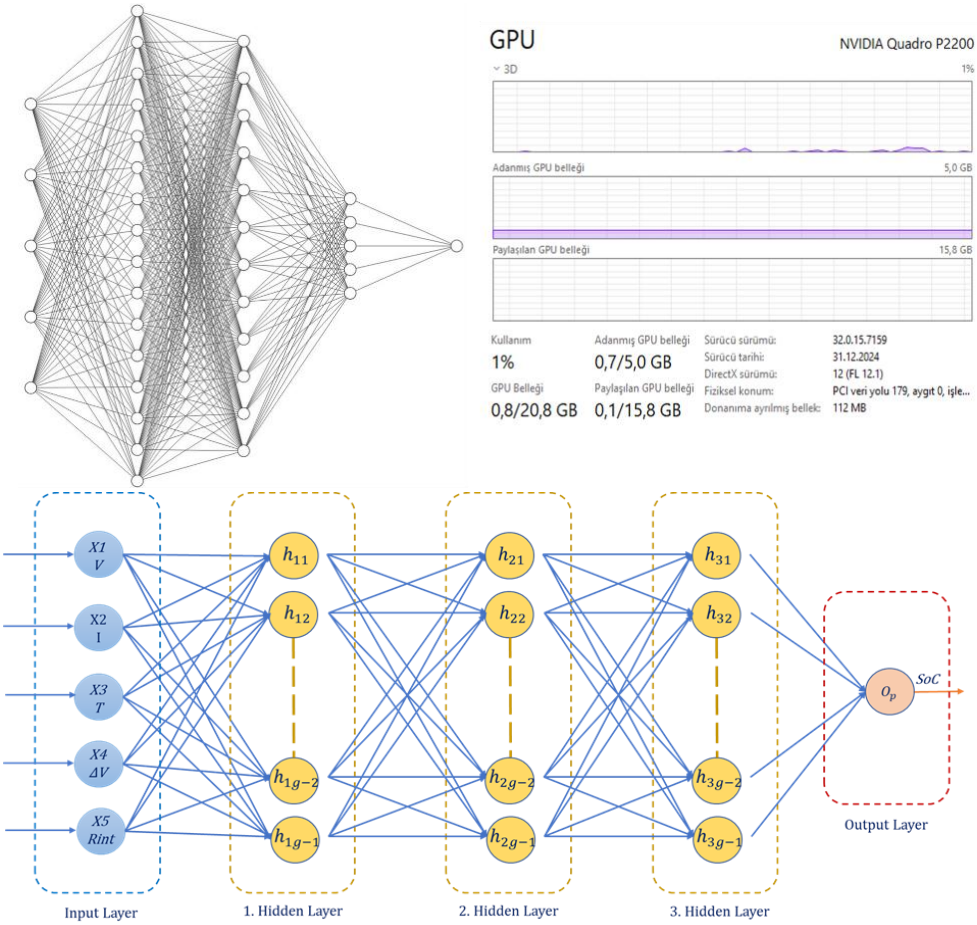

Figure 8 Proposed DNN architecture

3. Results

The HPPC test served as the experimental foundation for analyzing the dynamic electrochemical behavior of the Li-ion battery pack and for generating training data for the proposed deep neural network (DNN)–based SOC estimator. The HPPC procedure was conducted at predefined SOC intervals ranging from 100% to 10% in 10% decrements, with each segment initiated through precise coulomb counting to ensure accurate reference SOC control (Lelie et al., 2018). The immediate voltage drops followed by relaxation toward steady-state revealed the polarization characteristics, from which the open-circuit voltage (OCV) corresponding to each SOC level was determined (Jumah et al., 2022). The derived OCV–SOC relationship demonstrated a nonlinear yet monotonic behavior, characterized by pronounced gradients at both low and high SOC regions. Based on the HPPC profiles, key parameters were extracted and integrated into the DNN input feature set to enhance its capacity for modeling complex nonlinear interactions among voltage, current, temperature, and SOC as shown in the following Figure 9.

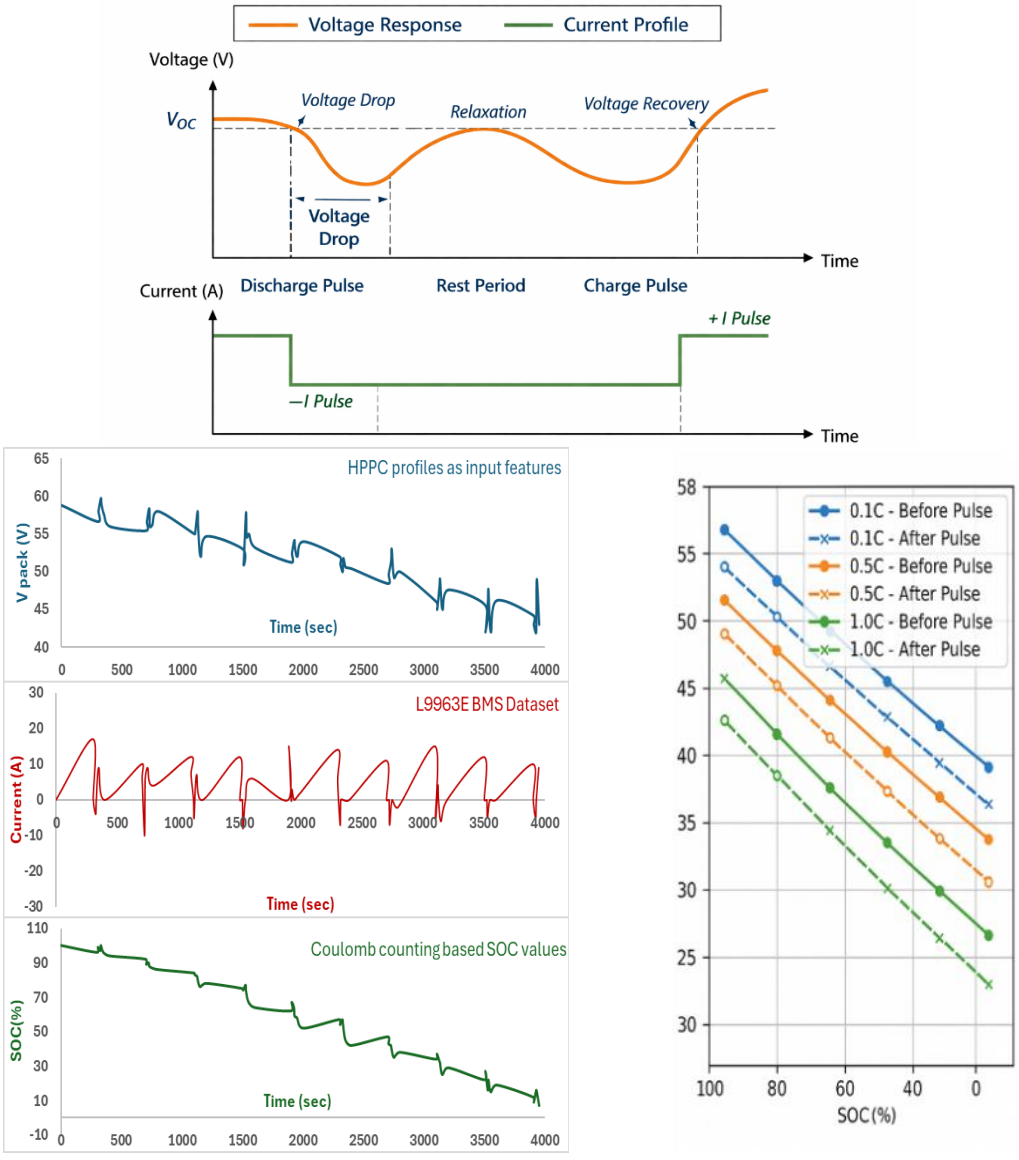

Figure 9 HPPC illustration and derived extracted features

Within each test interval, a predefined sequence of discharge current pulses was applied to characterize the transient electrochemical behavior of the battery. The resulting voltage and current responses were recorded and utilized as a preprocessing step for extracting key dynamic features, as illustrated in Figure 10.

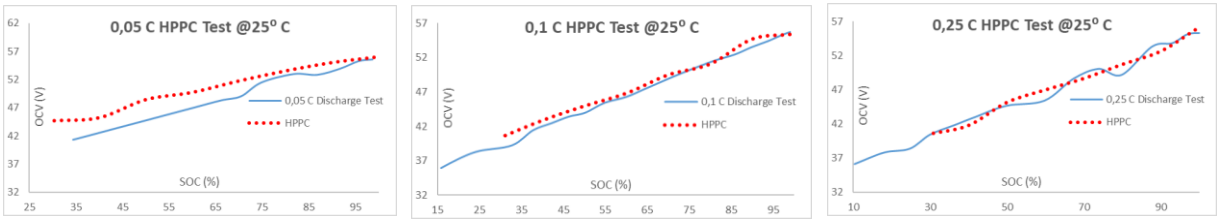

Figure 10 HPPC test profiles

The proposed DNN, trained exclusively on HPPC-derived data, was evaluated under the UDDS cycle without any retraining or fine-tuning to assess its extrapolation to real-world conditions. A comparative evaluation was performed against the traditional coulomb counting method under identical current load profiles. Quantitative results are summarized in Table 3. Even in low-dynamic regimes characterized by smooth current transitions, the DNN maintained higher precision by implicitly learning voltage–current–temperature correlations from HPPC data.

Table 3 Experimental results of HPPC derived augmented DNN

Root Mean Square Error (RMSE)	0.72%
Mean Absolute Error (MAE)	0.55%
R^2 Score	0.983

To evaluate thermal robustness, SOC estimation accuracy was assessed across four ambient temperatures (−20 °C to 50 °C) using the UDDS cycle. The proposed DNN closely tracked the reference SOC with minimal deviation, even during rapid transient conditions. Despite these challenges, the DNN consistently outperformed coulomb counting, which exhibited nearly double the estimation error at low temperatures. At elevated temperature (50 °C), the DNN achieved its best performance (MAE = 1.46%), demonstrating strong adaptability and stability under thermal stress. Table 4 summarizes the performance results, while Figure 11 presents the training and testing outcomes, comparing actual and predicted SOC profiles across a wide temperature range.

Table 4. MAE comparison of SOC estimation methods across operating conditions - Performance results summary

Temperature ◦C	DNN MAE (%)	Coulomb Counting MAE (%)
-20	2.1	4.21
0	1.92	4.05
25	1.56	3.95
50	1.46	3.1

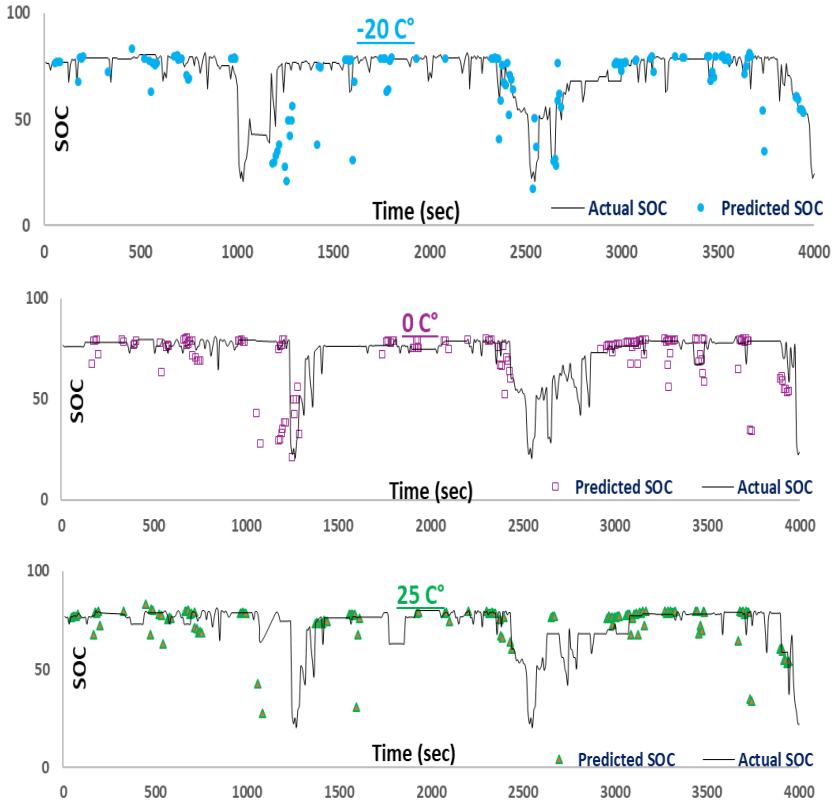

Figure 11 Training test results

This robust performance across diverse environmental and load conditions stems from the DNN's capacity to internalize latent correlations among temperature, current, and voltage during training. Unlike model-based estimators, it does not depend on explicit thermal modeling or parameter tuning, enabling effective operation in previously unseen conditions. Overall, the integration of HPPC-derived electrochemical features with deep learning produced a hybrid, feature-augmented SOC estimator capable of accurate and thermally consistent performance by addressing key limitations of conventional model-based and coulomb-counting approaches.

4. Discussion

The proposed feedforward deep neural network (DNN), trained exclusively on HPPC data, exhibited exceptional accuracy and robustness in SOC estimation for a 14-cell lithium-ion battery pack. The model achieved a mean squared error (MSE) of approximately 3×10^{-4}, a mean absolute error (MAE) of 0.015 (corresponding to a 1.5% SOC deviation), and a coefficient of determination (R^2) exceeding 0.98 across all dynamic test conditions. These results confirm the network's strong ability to capture complex, nonlinear interactions among voltage, current, temperature, and internal resistance that govern electrochemical behavior under varying loads. The close correspondence between predicted and reference SOC trajectories—with only minor deviations during abrupt current transients—demonstrates the model's capacity to maintain accuracy across rapid, high-frequency variations that often challenge conventional estimators.

The model's ability to generalize was further validated using the UDDS profiles. Despite being trained under quasi-static laboratory conditions, the DNN successfully extrapolated to real-world transient driving scenarios, maintaining high prediction accuracy. This result highlights the representational richness of HPPC data, which encapsulate essential electrochemical dynamics sufficient to approximate field

conditions when coupled with appropriate preprocessing and normalization. Such transferability is of notable practical importance, as it reduces the need for extensive field data collection for DNN training.

Nevertheless, certain limitations warrant further exploration. The current feedforward architecture does not explicitly model temporal dependencies, which may limit its capability to capture long-term state evolution under extended dynamic or irregular load profiles. Moreover, the model assumes stationary electrochemical behavior and does not explicitly account for degradation processes such as capacity fade, resistance growth, or lithium plating—factors that may alter OCV–SOC and impedance characteristics over time. Incorporating online or adaptive retraining mechanisms could mitigate long-term estimation drift and maintain accuracy throughout the battery's service life.

Future work will extend this framework toward hybrid, physics-informed architectures. Incorporating recurrent structures such as Long Short-Term Memory (LSTM) or Temporal Convolutional Networks (TCN) will enable explicit temporal modeling of SOC dynamics, while integrating state-of-health (SOH) estimation modules could facilitate concurrent monitoring of degradation behavior for predictive maintenance. From an implementation standpoint, deploying the trained model in real-time BMS will require further investigation into computational efficiency, quantization robustness, and interpretability.

In summary, deep learning models enhanced with HPPC-derived electrochemical features effectively bridge the gap between data-driven and physics-based approaches. The proposed framework delivers accurate, drift-free, and thermally consistent SOC estimation under dynamic conditions, providing a viable pathway toward next-generation adaptive and self-learning BMS architectures.

5. Conclusion

This study presented a comprehensive framework for accurate and robust SOC estimation in lithium-ion batteries by coupling the HPPC protocol with a deep learning–based modeling approach. The proposed feedforward deep neural network (DNN), trained on HPPC-derived voltage, current, temperature, and resistance features, effectively captured the nonlinear electrochemical dynamics governing battery behavior across diverse operating conditions. Spanning temperatures from −20 °C to 50 °C and C-rates from 0.05C to 0.25C, the model achieved a mean absolute error (MAE) of 1.5%, mean squared error (MSE) of 0.0003, and a coefficient of determination (R^2) above 0.98—demonstrating superior predictive fidelity relative to traditional estimation techniques.

Compared with conventional coulomb counting, the DNN exhibited substantially improved accuracy, generalization, and noise resilience. Its reliable performance across a 14-cell configuration managed by the L9963E BMS confirms its scalability and practical suitability for embedded applications. Furthermore, the network successfully learned key dynamic behaviors—including voltage recovery, hysteresis, and polarization—phenomena often difficult to model analytically. These findings highlight the HPPC protocol as an information-rich and standardized foundation for developing machine learning–based estimators that enhance electrochemical interpretability.

Beyond methodological contributions, this work advances the broader pursuit of intelligent and adaptive BMS architectures. Integrating AI-driven estimation within systems such as the L9963E enhances diagnostic reliability, predictive control, and operational safety in electric vehicles and stationary energy storage. The model's demonstrated ability to generalize from controlled HPPC laboratory datasets to complex real-world driving profiles underscores the transformative potential of hybrid experimental–machine learning frameworks for next-generation energy management systems.

Nevertheless, opportunities for improvement remain. The present DNN architecture does not explicitly model temporal dependencies or account for progressive degradation, which may affect long-term estimation accuracy. Future work will focus on incorporating recurrent networks—such as LSTM or Gated Recurrent Unit (GRU) architectures—to capture time-correlated SOC dynamics, as well as coupling SOC estimation with SOH prediction for aging-aware performance. Additionally, hybrid physics-informed

approaches, potentially implemented through digital-twin paradigms, could enhance model interpretability and enable adaptive recalibration under evolving electrochemical states.

In conclusion, this research establishes a scalable, high-fidelity, and data-centric methodology for SOC estimation, effectively bridging the domains of experimental electrochemistry and artificial intelligence. By embedding HPPC-informed deep learning models into intelligent BMS platforms, the proposed framework paves the way toward self-learning, adaptive, and resilient energy storage systems—advancing the reliability, safety, and sustainability of future electric mobility and renewable energy infrastructures (Miao et al., 2022).

Declaration of Ethical Standards

As the authors of this study, we declare that he complies with all ethical standards.

Credit Authorship Contribution Statement

A. Mühendis: Software, Validation, Formal analysis, Writing -Original Draft, Visualization.

R. Akkaya: Investigation, Resources, Writing, Review & Editing, Supervision, Funding acquisition.

Declaration of Competing Interest

The authors declared that they have no conflict of interest.

Funding / Acknowledgements

This study has been supported by Konya Technical University/Scientific Research Projects (BAP) Coordination Office in frame of the project code of 231102057.

Data Availability

The datasets are available.

References

Carrera, R., Quiroz, L., Guevara, C., & Acosta-Vargas, P. (2025). State-of-Charge Estimation of Medium- and High-Voltage Batteries Using LSTM Neural Networks Optimized with Genetic Algorithms. *Sensors*, *25*(15), 4632. https://doi.org/10.3390/s25154632

Chandran, V., Patil, C. K., Karthick, A., Ganeshaperumal, D., Rahim, R., & Ghosh, A. (2021). State of charge estimation of lithium-ion battery for electric vehicles using machine learning algorithms. *World Electric Vehicle Journal*, *12*(1). https://doi.org/10.3390/wevj12010038

Dai, H., Jiang, B., Hu, X., Lin, X., Wei, X., & Pecht, M. (2021a). Advanced battery management strategies for a sustainable energy future: Multilayer design concepts and research trends. In *Renewable and Sustainable Energy Reviews* (Vol. 138). Elsevier Ltd. https://doi.org/10.1016/j.rser.2020.110480

Dai, H., Jiang, B., Hu, X., Lin, X., Wei, X., & Pecht, M. (2021b). Advanced battery management strategies for a sustainable energy future: Multilayer design concepts and research trends. In *Renewable and Sustainable Energy Reviews* (Vol. 138). Elsevier Ltd. https://doi.org/10.1016/j.rser.2020.110480

El Fallah, S., Kharbach, J., Vanagas, J., Vilkelytė, Ž., Tolvaišienė, S., Gudžius, S., Kalvaitis, A., Lehmam, O., Masrour, R., Hammouch, Z., Rezzouk, A., & Ouazzani Jamil, M. (2024). Advanced State of Charge Estimation Using Deep Neural Network, Gated Recurrent Unit, and Long Short-Term Memory Models for Lithium-Ion Batteries under Aging and Temperature Conditions. *Applied Sciences (Switzerland)*, *14*(15). https://doi.org/10.3390/app14156648

El Maliki, A., Anoune, K., Benlafkih, A., & Hadjoudja, A. (2024). Estimating the state of charge of lithium-ion batteries using different noise inputs. *International Journal of Power Electronics and Drive Systems*, *15*(1), 8–18. https://doi.org/10.11591/ijpeds.v15.i1.pp8-18

Eleftheriadis, P., Giazitzis, S., Leva, S., & Ogliari, E. (2023). Data-Driven Methods for the State of Charge Estimation of Lithium-Ion Batteries: An Overview. In *Forecasting* (Vol. 5, Number 3, pp. 576–599). Multidisciplinary Digital Publishing Institute (MDPI). https://doi.org/10.3390/forecast5030032

Fang, Y., Zhang, Q., Zhang, H., Xu, W., Wang, L., Shen, X., Yun, F., Cui, Y., Wang, L., & Zhang, X. (2021). State-of-charge estimation technique for lithium-ion batteries by means of second-order extended Kalman filter and equivalent circuit model: Great temperature robustness state-of-charge estimation. *IET Power Electronics*, *14*(8),

1515–1528. https://doi.org/10.1049/pel2.12129

Frendo, O., Graf, J., Gaertner, N., & Stuckenschmidt, H. (2020). Data-driven smart charging for heterogeneous electric vehicle fleets. *Energy and AI*, *1*. https://doi.org/10.1016/j.egyai.2020.100007

Ghaeminezhad, N., Ouyang, Q., Wei, J., Xue, Y., & Wang, Z. (2023). Review on state of charge estimation techniques of lithium-ion batteries: A control-oriented approach. In *Journal of Energy Storage* (Vol. 72). Elsevier Ltd. https://doi.org/10.1016/j.est.2023.108707

Hannan, M. A., Lipu, M. S. H., Hussain, A., Ker, P. J., Mahlia, T. M. I., Mansor, M., Ayob, A., Saad, M. H., & Dong, Z. Y. (2020). Toward Enhanced State of Charge Estimation of Lithium-ion Batteries Using Optimized Machine Learning Techniques. *Scientific Reports*, *10*(1). https://doi.org/10.1038/s41598-020-61464-7

Harper, G. D. J., Kendrick, E., Anderson, P. A., Mrozik, W., Christensen, P., Lambert, S., Greenwood, D., Das, P. K., Ahmeid, M., Milojevic, Z., Du, W., Brett, D. J. L., Shearing, P. R., Rastegarpanah, A., Stolkin, R., Sommerville, R., Zorin, A., Durham, J. L., Abbott, A. P., … Boons, F. (2023). Roadmap for a sustainable circular economy in lithium-ion and future battery technologies. *JPhys Energy*, *5*(2). https://doi.org/10.1088/2515-7655/acaa57

Hossain Lipu, M. S., Hannan, M. A., Hussain, A., Ayob, A., Saad, M. H. M., Karim, T. F., & How, D. N. T. (2020). Data-driven state of charge estimation of lithium-ion batteries: Algorithms, implementation factors, limitations and future trends. In *Journal of Cleaner Production* (Vol. 277). Elsevier Ltd. https://doi.org/10.1016/j.jclepro.2020.124110

Hu, X., Feng, F., Liu, K., Zhang, L., Xie, J., & Liu, B. (2019). State estimation for advanced battery management: Key challenges and future trends. In *Renewable and Sustainable Energy Reviews* (Vol. 114). Elsevier Ltd. https://doi.org/10.1016/j.rser.2019.109334

JiaQi, Z., DeXin, G., YuanMing, C., & Qing, Y. (2024). A new method for thermal runaway warning of electric vehicle charging. *Measurement Science and Technology*, *35*(12). https://doi.org/10.1088/1361-6501/ad7e47

Jin, S., Sui, X., Huang, X., Wang, S., Teodorescu, R., & Stroe, D. I. (2021). Overview of machine learning methods for lithium-ion battery remaining useful lifetime prediction. *Electronics (Switzerland)*, *10*(24). https://doi.org/10.3390/electronics10243126

Jumah, S., Elezab, A., Zayed, O., Ahmed, R., Narimani, M., & Emadi, A. (2022). State of Charge Estimation for EV Batteries Using Support Vector Regression. *2022 IEEE Transportation Electrification Conference and Expo, ITEC 2022*, 964–969. https://doi.org/10.1109/ITEC53557.2022.9813811

Ko, Y., & Choi, W. (2021). A new soc estimation for lfp batteries: Application in a 10 ah cell (hw 38120 l/s) as a hysteresis case study. *Electronics (Switzerland)*, *10*(6), 1–14. https://doi.org/10.3390/electronics10060705

Lelie, M., Braun, T., Knips, M., Nordmann, H., Ringbeck, F., Zappen, H., & Sauer, D. U. (2018). Battery management system hardware concepts: An overview. *Applied Sciences (Switzerland)*, *8*(4). https://doi.org/10.3390/app8040534

Liu, F., Liu, T., & Fu, Y. (2016). An Improved SoC Estimation Algorithm Based on Artificial Neural Network. *Proceedings - 2015 8th International Symposium on Computational Intelligence and Design, ISCID 2015*, *2*, 152–155. https://doi.org/10.1109/ISCID.2015.2

Liu, W., Placke, T., & Chau, K. T. (2022a). Overview of batteries and battery management for electric vehicles. In *Energy Reports* (Vol. 8, pp. 4058–4084). Elsevier Ltd. https://doi.org/10.1016/j.egyr.2022.03.016

Liu, W., Placke, T., & Chau, K. T. (2022b). Overview of batteries and battery management for electric vehicles. In *Energy Reports* (Vol. 8, pp. 4058–4084). Elsevier Ltd. https://doi.org/10.1016/j.egyr.2022.03.016

Majasan, J. O., Robinson, J. B., Owen, R. E., Maier, M., Radhakrishnan, A. N. P., Pham, M., Tranter, T. G., Zhang, Y., Shearing, P. R., & Brett, D. J. L. (2021). Recent advances in acoustic diagnostics for electrochemical power systems. In *JPhys Energy* (Vol. 3, Number 3). IOP Publishing Ltd. https://doi.org/10.1088/2515-7655/abfb4a

Miao, J., Tong, Z., Tong, S., Zhang, J., & Mao, J. (2022). State of Charge Estimation of Lithium-Ion Battery for Electric Vehicles under Extreme Operating Temperatures Based on an Adaptive Temporal Convolutional Network. *Batteries*, *8*(10). https://doi.org/10.3390/batteries8100145

Mühendis, A., & Akkaya, R. (n.d.-a). *Conference Book Comprehensive Review of Advanced Features and Diagnostic Tasks Analysis of L99615c Battery Management System*.

Mühendis, A., & Akkaya, R. (n.d.-b). *Review Of Artificial Intelligence Based Integration Techniques Of Battery Management System For Electric Vehicles*. Retrieved https://www.researchgate.net/publication/371762315

Mühendis, A., & Akkaya, R. (2025). Integrating Machine Learning with Advanced Features of L9963E BMS for Enhanced State of Charge Estimation. *International Journal of Automotive Science And Technology*, *9*(4), 475–490. https://doi.org/10.30939/ijastech..1698286

Mühendis, A., & Kulaksiz, A. A. (2020). Maksimum Güç Noktası İzleme Tekniklerinde Uygulanan LabVIEW Tabanlı

Modelleme Sistemi. *European Journal of Science and Technology*, 445–454. https://doi.org/10.31590/ejosat.809517

Murnane, M., & Ghazel, A. (n.d.). *A Closer Look at State of Charge (SOC) and State of Health (SOH) Estimation Techniques for Batteries*.

Naha, A., Han, S., Agarwal, S., Guha, A., Khandelwal, A., Tagade, P., Hariharan, K. S., Kolake, S. M., Yoon, J., & Oh, B. (2020). An Incremental Voltage Difference Based Technique for Online State of Health Estimation of Li-ion Batteries. *Scientific Reports*, *10*(1). https://doi.org/10.1038/s41598-020-66424-9

Obisakin, I., & Ekeanyanwu, C. V. (2022). State of Health Estimation of Lithium-Ion Batteries Using Support Vector Regression and Long Short-Term Memory. *Open Journal of Applied Sciences*, *12*(08), 1366–1382. https://doi.org/10.4236/ojapps.2022.128094

Obuli Pranav, D., Babu, P. S., Indragandhi, V., Ashok, B., Vedhanayaki, S., & Kavitha, C. (2024). Enhanced SOC estimation of lithium ion batteries with RealTime data using machine learning algorithms. *Scientific Reports*, *14*(1). https://doi.org/10.1038/s41598-024-66997-9

Pop, V., Bergveld, H. J., Notten, P. H. L., & Regtien, P. P. L. (2005). State-of-the-art of battery state-of-charge determination. In *Measurement Science and Technology* (Vol. 16, Number 12). Institute of Physics Publishing. https://doi.org/10.1088/0957-0233/16/12/R01

Ren, H., Zhao, Y., Chen, S., & Wang, T. (2019a). Design and implementation of a battery management system with active charge balance based on the SOC and SOH online estimation. *Energy*, *166*, 908–917. https://doi.org/10.1016/j.energy.2018.10.133

Ren, H., Zhao, Y., Chen, S., & Wang, T. (2019b). Design and implementation of a battery management system with active charge balance based on the SOC and SOH online estimation. *Energy*, *166*, 908–917. https://doi.org/10.1016/j.energy.2018.10.133

Ren, Z., & Du, C. (2023). A review of machine learning state-of-charge and state-of-health estimation algorithms for lithium-ion batteries. In *Energy Reports* (Vol. 9, pp. 2993–3021). Elsevier Ltd. https://doi.org/10.1016/j.egyr.2023.01.108

Tong, S., Lacap, J. H., & Park, J. W. (2016). Battery state of charge estimation using a load-classifying neural network. *Journal of Energy Storage*, *7*, 236–243. https://doi.org/10.1016/j.est.2016.07.002

Tran, M. K., Panchal, S., Khang, T. D., Panchal, K., Fraser, R., & Fowler, M. (2022). Concept Review of a Cloud-Based Smart Battery Management System for Lithium-Ion Batteries: Feasibility, Logistics, and Functionality. In *Batteries* (Vol. 8, Number 2). MDPI. https://doi.org/10.3390/batteries8020019

Wang, S., Jia, X., Takyi-Aninakwa, P., Stroe, D.-I., & Fernandez, C. (2023). Review—Optimized Particle Filtering Strategies for High-Accuracy State of Charge Estimation of LIBs. *Journal of The Electrochemical Society*, *170*(5), 050514. https://doi.org/10.1149/1945-7111/acd148

Wassiliadis, N., Schneider, J., Frank, A., Wildfeuer, L., Lin, X., Jossen, A., & Lienkamp, M. (2021). Review of fast charging strategies for lithium-ion battery systems and their applicability for battery electric vehicles. In *Journal of Energy Storage* (Vol. 44). Elsevier Ltd. https://doi.org/10.1016/j.est.2021.103306

Wu, J., Wang, Y., Zhang, X., & Chen, Z. (2016). A novel state of health estimation method of Li-ion battery using group method of data handling. *Journal of Power Sources*, *327*, 457–464. https://doi.org/10.1016/j.jpowsour.2016.07.065

Xiao, Y., Song, W., Liu, W., & Wan, F. (2024). Estimation of lithium battery state of charge using the LTG-SABO-GRU model. *Measurement Science and Technology*, *35*(11). https://doi.org/10.1088/1361-6501/ad69b3

Xiong, R., Cao, J., Yu, Q., He, H., & Sun, F. (2017). Critical Review on the Battery State of Charge Estimation Methods for Electric Vehicles. *IEEE Access*, *6*, 1832–1843. https://doi.org/10.1109/ACCESS.2017.2780258

Yang, B., Wang, J., Cao, P., Zhu, T., Shu, H., Chen, J., Zhang, J., & Zhu, J. (2021). Classification, summarization and perspectives on state-of-charge estimation of lithium-ion batteries used in electric vehicles: A critical comprehensive survey. In *Journal of Energy Storage* (Vol. 39). Elsevier Ltd. https://doi.org/10.1016/j.est.2021.102572

Yuan, N., Mao, R., Han, P., Xu, W., Li, Y., Guo, Y., & Zhang, H. (2025). A dual-exponential EKF model for lithium-ion battery RUL prediction with Bayesian optimization. *Measurement Science and Technology*, *36*(9). https://doi.org/10.1088/1361-6501/ae00e6

Zheng, M., & Luo, X. (2024). Joint estimation of State of Charge (SOC) and State of Health (SOH) for lithium ion batteries using Support Vector Machine (SVM), Convolutional Neural Network (CNN) and Long Sort Term Memory Network (LSTM) models. *International Journal of Electrochemical Science*, *19*(9). https://doi.org/10.1016/j.ijoes.2024.100747